Interaction of ion clusters with fusion plasmas: Scaling laws

N. R. Arista and E. M. Bringa
División Colisiones Atómicas, Centro Atómico Bariloche, Instituto Balseiro, 8400 Bariloche, Argentina
(Received 3 June 1996; revised manuscript received 5 November 1996)

The interaction between large ion clusters or very intense ion beams with fusion plasma is studied using the dielectric function formalism with appropriate quantum corrections. The contributions from individual and collective modes to the energy loss are calculated. The general properties of the interference effects are characterized in terms of the relevant parameters, and simple scaling laws are obtained. In particular, the conditions for a maximum enhancement in the energy deposition are derived. The study provides a unified view and a general formulation of collective effects in the energy loss for low and high velocities of the beam particles. [S1050-2947(97)02104-5]

PACS number(s): 34.50.Bw, 52.40.Mj

I. INTRODUCTION

The interaction of energetic ion beams with dense and dilute plasmas is one of the fundamental processes in plasma physics and fusion studies. The research in this area includes relevant applications to magnetically confined (MCF) and inertially confined (ICF) fusion.

In particular, the use of intense atomic beams provides a very effective method to reach the high temperatures required to approach break-even conditions in tokamak systems [1,2]. Recently, interest has focused also on the application of pulsed beams of ions or atomic clusters in ICF studies [3–6], after the main advantages of this method were demon

strated, in particular with regards to an efficient beam-target coupling, with the possibility of adjusting the energy deposition profiles to obtain high energy concentrations and fast repetition rates [3–6].

On the other hand, the existence of interference effects in the interaction of swift clusters of ions with matter has been known for some time, for the case of both solid [7–10] and plasma targets [11–13]. According to recent estimates [14–16], consideration of collective effects arising from the simultaneous interaction of various ions with the plasma electrons may be relevant to account for the energy loss of very intense ion beams or clusters with plasmas. In a previous paper [17] we have studied the way in which collective interactions can modify the energy deposition in the medium, including several cases dealing with dense and dilute plasmas. We have found that under appropriate conditions the coherent interaction of large clusters with the plasma can produce a significant enhancement of the energy loss.

The purpose of this paper is to provide a more general approach to this problem, using a theoretical framework that applies to nearly all the cases of experimental interest. The developments are based on the classical dielectric function formalism with appropriate quantum corrections. Useful approximations will be made in order to integrate the interference effects for large clusters of particles. The results will be described in terms of a few scaling functions which depend on the main parameters of the beam and the system.

The formulation is described in Sec. II and Sec. III contains calculations for several illustrative cases. The general properties and scaling relations are studied in Sec. IV, and the main conclusions are summarized in Sec. V.

II. FORMULATION

A. Main parameters

The main parameters in the problem of particle-plasma interaction are the particle charge Z, its velocity v, the plasma density n_p, and temperature T. In addition, for correlated ions one should include the internuclear distances r_{ij} in order to describe interference effects.

Other quantities of interest are the plasma frequency ω_p, thermal electron velocity v_T, and Debye length λ_D, given by (atomic units will be used throughout this paper)

$$\omega_p=\sqrt{4\pi n_p},\quad v_T=\sqrt{k_BT},\quad \lambda_D=v_T/\omega_p=\sqrt{k_BT/4\pi n_p}. \tag{1}$$

The value of λ_D is representative of the interaction between slow ions (i.e., $v<v_T$). The screening in this case may be represented by a Yukawa potential with a screening distance λ_D, and so the interaction between slow ions will be significant only for distances $r<\lambda_D$.

On the other hand, in the case of swift ions ($v>v_T$) the induced perturbation spreads over a more extended range, of the order of the dynamical screening length,

$$\lambda(v)=\frac{v}{\omega_p}=\frac{\lambda_W}{2\pi}, \tag{2}$$

related to the so-called *wake* length $\lambda_W=2\pi v/\omega_p$, which is the characteristic wavelength of the oscillatory perturbation produced behind the particle trajectory [18]; this process is due to collective phenomena induced in the medium (i.e., plasma waves or plasmon excitations), and in this case the dominant mechanism of energy exchange is given by long-range interactions (with $r\sim\lambda_W$) between separated ions.

The characteristics of the interactions between pairs of correlated ions in plasmas have been discussed in detail in a previous paper [19].

B. Energy loss of ion clusters

According to the dielectric formulation, the mean energy loss for a cluster of N ions with charges Z_i and positions $\vec{r}_i$ can be separated as follows [9]:

$$S_{\rm cl}=\left\langle -\frac{dE}{dx}\right\rangle=\sum_{i=1}^{N} Z_i^2 S_0(v)+\sum_{i\neq j} Z_i Z_j I(\vec{r}_{ij},\vec{v}), \quad (3)$$

where $S_0(v)$ is the usual stopping power of single ions, and $I(\vec{r}_{ij},\vec{v})$ denote the interference term for a pair of correlated ions, with internuclear distance $\vec{r}_{ij}=\vec{r}_i-\vec{r}_j$. The values of $S_0(v)$ and $I(\vec{r}_{ij},\vec{v})$ are given, in terms of the longitudinal dielectric function $\epsilon(k,\omega)$ (nonrelativistic velocities are considered) by [9]

$$S_0(v)=\frac{1}{2\pi^2 v}\int d^3k\left(\frac{\vec{k}\cdot\vec{v}}{k^2}\right)\mathrm{Im}\left[\frac{-1}{\epsilon(k,\omega)}\right], \quad (4)$$

$$I(\vec{r},\vec{v})=\frac{1}{2\pi^2 v}\int d^3k\left(\frac{\vec{k}\cdot\vec{v}}{k^2}\right)\mathrm{Im}\left[\frac{-1}{\epsilon(k,\omega)}\right]\cos(\vec{k}\cdot\vec{r}), \quad (5)$$

with $\omega=\vec{k}\cdot\vec{v}$.

It should be noted that the present description does not include the energy losses that may arise from the excitation or ionization of bound electrons in the moving ions, and we assume that the ions have reached a state of charge equilibrium with the medium [1,4,14]. We shall assume also that all the ions move with the same velocity $\vec{v}$.

The obvious limits of Eq. (5) are the following: (i) for $\vec{r}_{ij}=0$: $I(\vec{r}_{ij},\vec{v})=S_0$, and $S_{\rm cl}=(\Sigma_{i=1}^{N}Z_i)^2 S_0$, and (ii) for $\vec{r}_{ij}\to\infty$: $I(\vec{r}_{ij},\vec{v})\to 0$, and $S_{\rm cl}=(\Sigma_{i=1}^{N}Z_i^2)S_0$. The first case corresponds to the limit of united ions, and the second to a collection of uncorrelated ions.

In the case of homonuclear clusters, $Z_i=Z_j=Z$, to be considered here, we can simplify the previous expressions as follows:

$$S_{\rm cl}=NZ^2[S_0(v)+I_{\rm cl}(\vec{v})], \quad (6)$$

where $I_{\rm cl}(\vec{v})$ is the averaged interference function for the whole cluster, defined by

$$I_{\rm cl}(\vec{v})=\frac{1}{N}\sum_{i\neq j} I(\vec{r}_{ij},\vec{v}). \quad (7)$$

C. Cluster model

The case of atomic and molecular clusters interacting with dense media has been considered in detail by Abril *et al.* [20] taking into account the internal correlations among the particles in the cluster. It was shown that a satisfactory representation of spherical clusters may be obtained with a rather simple model, where the internal correlations are represented, in an average way, by introducing a correlation (or exclusion) volume of radius r_0 around each ion in the cluster. In addition, the effect of the finite size of a cluster of radius $r_{\rm cl}$ may be incorporated in a statistical function $p(r)$, which takes into account, also in average, the decreasing effective number of neighbors at larger distances r within the cluster [20] [in particular, $p(r)=0$ when $r\geqslant 2r_{\rm cl}$].

According to this model, the *pair correlation function* $g_{\rm cl}(r)$ for a cluster of N ions with radius $r_{\rm cl}$ may be written in terms of the correlation function for an infinite system $g_0(r)$ as follows:

$$g_{\rm cl}(r)=C_N g_0(r) p\left(\frac{r}{2r_{\rm cl}}\right), \quad (8)$$

where

$$p(x)=\begin{cases}1-\frac{3}{2}x+\frac{1}{2}x^3, & x<1\\ 0, & x\geqslant 1\end{cases} \quad (9)$$

and $x=r/2r_{\rm cl}$.

Following Ref. [20], the function $g_0(r)$ will be taken as constant for distances larger than the correlation-hole radius r_0, namely,

$$g_0(r)=\begin{cases}0, & r<r_0\\ 1, & r>r_0.\end{cases} \quad (10)$$

The value of the constant C_N is obtained from the normalization condition:

$$n_{\rm cl}\int d^3r\, g_{\rm cl}(r)=N-1, \quad (11)$$

where $n_{\rm cl}$ is the density of particles in the cluster.

From Eqs. (8)–(11) one finds

$$C_N(x_0)=\left(\frac{N-1}{N}\right)\left(\frac{1}{1-8x_0^3+9x_0^4-2x_0^6}\right),$$

$$\text{with } x_0=\left(\frac{r_0}{2r_{\rm cl}}\right). \quad (12)$$

In addition, the values of r_0 and $r_{\rm cl}$ are related to the density $n_{\rm cl}$ by

$$\frac{4\pi}{3}r_0^3 n_{\rm cl}=1, \quad \frac{4\pi}{3}r_{\rm cl}^3 n_{\rm cl}=N, \quad (13)$$

and therefore $(r_{\rm cl}/r_0)^3=N$.

In particular, for $N\gg 1$, we get $C_N\to 1$, as should be expected.

D. Cluster integration

We can now express the value of $I_{\rm cl}$ by transforming the sum in Eq. (7) into an integral, taking into account the correlation effects described by $g_{\rm cl}(r)$, as follows:

$$I_{\rm cl}=n_{\rm cl}\int d^3r\; g_{\rm cl}(r) I(r,v), \quad (14)$$

where the interference term $I(r,v)$ may be written, after performing the angular average in Eq. (5), in the form [9]

$$I(r,v)=\frac{2}{\pi v^2}\int\frac{dk}{k}\int_0^{kv}\omega\, d\omega\ \mathrm{Im}\left[\frac{-1}{\epsilon(k,\omega)}\right]\frac{\sin(kr)}{kr}, \tag{15}$$

and a similar expression is obtained for $S_0(v)$, with $\sin(kr)/(kr)$ replaced by 1. The stopping power for the whole cluster is given by Eq. (6).

From Eqs. (14) and (15) we can also write

$$I_{\mathrm{cl}}=\frac{2}{\pi v^2}\int\frac{dk}{k}F_{\mathrm{cl}}(k)\int_0^{kv}\omega\, d\omega\ \mathrm{Im}\left[\frac{-1}{\epsilon(k,\omega)}\right], \tag{16}$$

where $F_{\mathrm{cl}}(k)$ is given by

$$F_{\mathrm{cl}}(k)=n_{\mathrm{cl}}\int d^3r\ g_{\mathrm{cl}}(r)\frac{\sin(kr)}{kr}. \tag{17}$$

Using now the model of Eqs. (8)–(12) for the pair correlation function, we get

$$I_{\mathrm{cl}}=4\pi n_{\mathrm{cl}}(2r_{\mathrm{cl}})^3C_N\int_{r_0}^{2r_{\mathrm{cl}}}\frac{dr}{2r_{\mathrm{cl}}}P(r/2r_{\mathrm{cl}})I(r,v), \tag{18}$$

where

$$P(x)=x^2p(x), \tag{19}$$

in terms of the function $p(x)$ of Eq. (9), with $x=r/2r_{\mathrm{cl}}$.

We show in Fig. 1 the function of interest for the integration of I_{cl} in Eq. (18), namely, $P(x)I(r,v)$, for two typical cases of low [Fig. 1(a)] and high [Fig. 1(b)] velocities. We show the behavior of this function in case (a) for $r_{\mathrm{cl}}=2\lambda_D$ and $r_{\mathrm{cl}}=10\lambda_D$, and in case (b) for $r_{\mathrm{cl}}=2v/\omega_P$ and $r_{\mathrm{cl}}=10v/\omega_P$. We notice an oscillatory behavior in the case of high velocities which is due to the function $I(r,v)$. As mentioned before, an important difference between the low- and the high-velocity cases arises from the different forms of the interaction between pairs of ions, produced, respectively, by the adiabatic and the dynamic response of the plasma electrons.

The integrations of the stopping and interference terms, $S_0(v)$ and $I(r,v)$, were performed as discussed in detail earlier [19], for the case of single and pairs of ions. The dielectric function for a classical (nondegenerate) plasma was parametrized as follows:

$$\epsilon(k,\omega)=1+\left(\frac{1}{k\lambda_D}\right)^2\Psi(z), \tag{20}$$

where $\Psi(z)\equiv X(z)+iY(z)$ is the plasma dispersion function [21] and $z=\omega/kv_T$.

The integrals over k in Eqs. (4) and (5) are restricted by an upper limit $k_{\max}$, given by the minimum between the quantum and the classical cutoff values (in a.u.):

$$k^q_{\max}=2(v+v_T),\quad k^{\mathrm{cl}}_{\max}=(v^2+v_T^2)/Z. \tag{21}$$

For light ions, $Z\sim1$, one usually finds that $k^q_{\max}<k^{\mathrm{cl}}_{\max}$; in this case the integration is independent of the ion charge and one can identify the value of S_0 with the proton stopping power S_p. For highly charged ions, the classical Bloch correction introduced by $k^{\mathrm{cl}}_{\max}$ produces a decrease of the stopping integral, so that $S_0<S_p$ (cf. [19,22]).

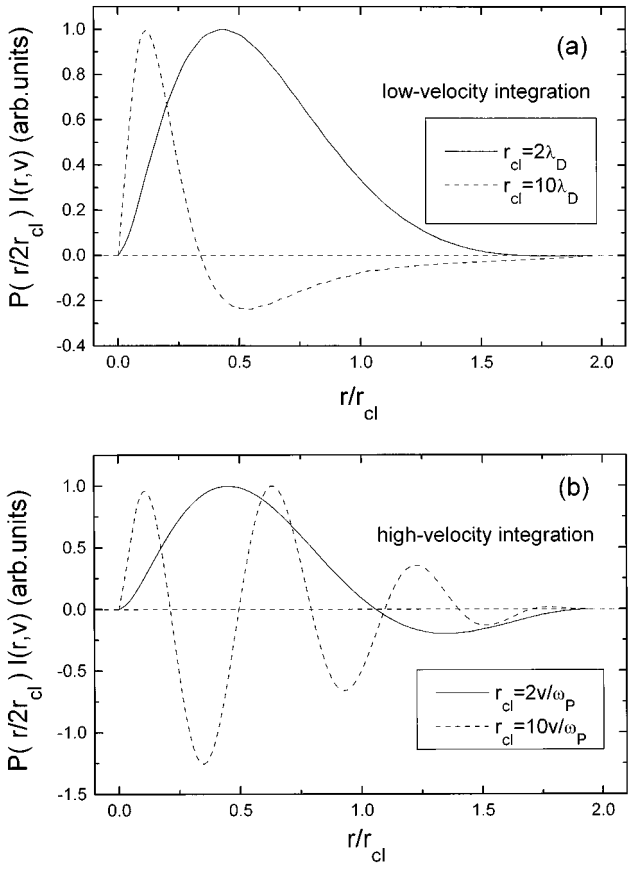

FIG. 1. Function $P(r/2r_{\mathrm{cl}})I(r,v)$ in the integral of Eq. (18), which determines the interference term for the whole cluster. In (a) we show two examples (with $r_{\mathrm{cl}}=2\lambda_D$ and $r_{\mathrm{cl}}=10\lambda_D$) corresponding to the low-velocity range, and in (b) we show two cases ($r_{\mathrm{cl}}=2v/\omega_P$ and $r_{\mathrm{cl}}=10v/\omega_P$) in the high-velocity range.

The separation of individual and collective excitations in the energy loss integrals has been discussed in Ref. [19], based on a detailed study of the plasma resonance frequencies in the complex plane. It is found that a simple way to separate both contributions is to consider the integrations in the ranges $0<k<k_D$ (collective modes) and $k_D<k<k_{\max}$ (individual modes), where $k_D=1/\lambda_D$.

III. CALCULATIONS

In order to demonstrate the main features of the vicinage and collective effects in the energy loss we studied the dependence of the interference term on velocity v, cluster radius r_{cl}, and correlation distance (or exclusion radius) r_0, for various plasma parameters in the range of interest for both ICF and MCF plasmas. Due to space limitations we will include here a few illustrative examples.

In Fig. 2, we show the velocity dependence of I_{cl} for a wide range of velocities. The results in this case depend very much on the exclusion radius (for r_0 in the range 200–500 a.u.) but not on cluster radius (for $r_{\mathrm{cl}}=10^3,10^5$, and 10^6 a.u.). This is due to the value of the main integration parameter: $r\omega_P/v$, which becomes very large for $r\sim r_{\mathrm{cl}}$.

A different situation is shown in Fig. 3. In this case the

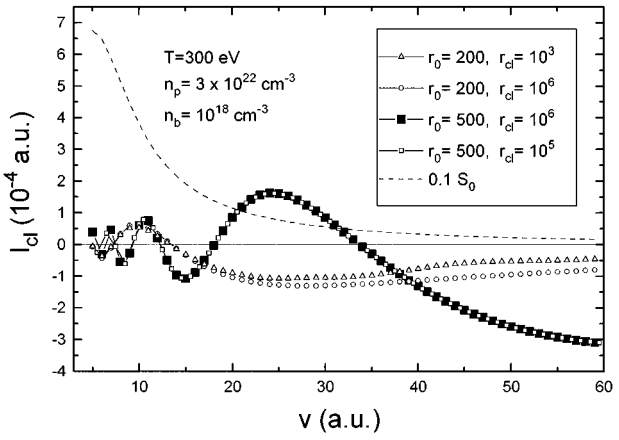

FIG. 2. Calculations of the interference term I_{cl} in Eq. (18) versus cluster velocity v for a dense plasma and for various cluster parameters r_0 and r_{cl} (in a.u.), as indicated in the inset.

interference term increases strongly with velocity, reaching a maximum at $v\sim 30$ a.u. Moreover, at large velocities (when $r_0\omega_P/v \ll 1$) the results become independent of the value of r_0.

A simple analysis helps to understand the difference between both behaviors. Thus, for example, for an intermediate velocity $v\sim 30$ a.u. (in the interval studied here) we find that the interaction range is of the order of $\lambda \equiv v/\omega_P \sim 130$ a.u. for the case of Fig. 2 (i.e., similar to the r_0 values), whereas in the case of Fig. 3 we get $\lambda \sim 2\times 10^4$ a.u. (similar to the r_{cl} value).

Therefore the oscillatory behavior in Fig. 2 is due to interferences arising from the interaction between close particles, with $r\sim r_0\sim\lambda$; this is the so-called *vicinage effect*. Instead, the maximum in Fig. 3 arises from a coherent interaction among many particles in the cluster, a process that becomes dominant when the dynamical interaction length λ is comparable to the cluster radius r_{cl}; this is then the *collective effect*, to be discussed in detail here.

Another question of interest is to show the relative contribution to the interference term I_{cl} of both the collective ($0<k<k_D$) and individual ($k_D<k<k_{\max}$) modes contained in the plasma response function [21].

To illustrate this point we show in Fig. 4 results obtained

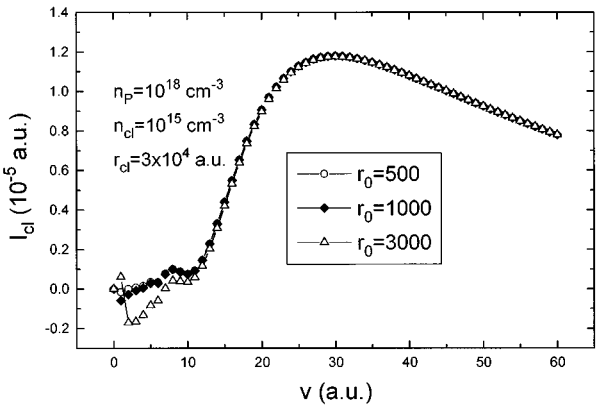

FIG. 3. Same as in Fig. 2, for $r_{\mathrm{cl}}=3\times 10^4$ and various values of r_0 (in a.u.).

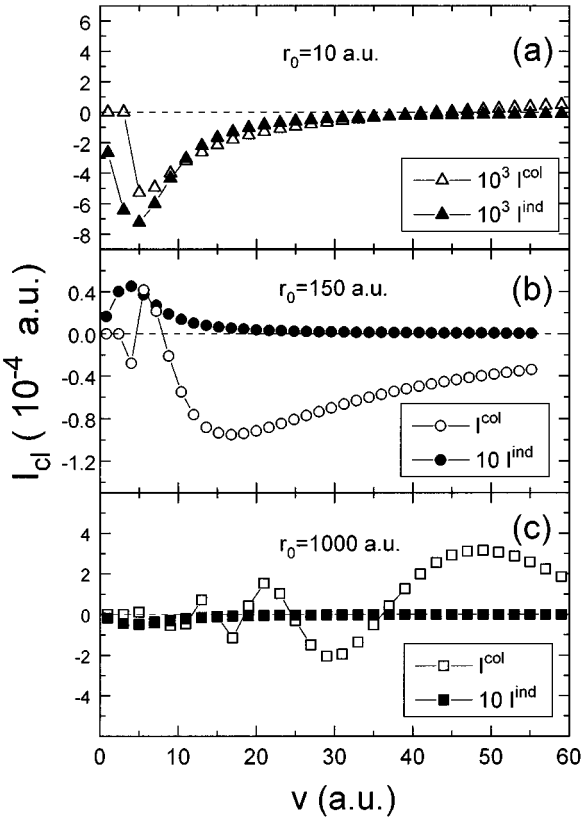

FIG. 4. Contributions to the interference term I_{cl} due to excitations of collective and individual modes in the plasma, for three values of the correlation radius r_0. The figure illustrates how collective modes become dominant for larger values of r_0 and for large velocities.

using the correlation radius r_0 as a free parameter (actually r_0 would be linked to the density of particles in the cluster n_{cl}), for the cases (a) $r_0=10$ a.u., (b) $r_0=150$ a.u., and (c) $r_0=1000$ a.u.

We find that for small values of r_0 [case (a)] the excitations of collective and individual modes are nearly equally important, but with increasing values of r_0 [cases (b) and (c)] the collective modes completely dominate the interferences. The first case ($r_0=10$) may be important for compact clusters incident on dense (ICF) plasmas, whereas the other cases ($r_0\sim$ 100–1000) may apply to ionized clusters exploding while penetrating dilute (MCF) plasmas. We also notice that the oscillations in the velocity dependence of I_{cl} become very important when r_0 matches the characteristic plasmon wavelength parameter λ_W.

IV. GENERAL PROPERTIES AND SCALING FUNCTIONS

Many of the results derived from this description can be analyzed in terms of the parameters introduced before. Therefore it seems worthwhile trying to express the main quantities in terms of a few scaling functions. This is the question that we will consider now.

Using the expression for the cluster stopping power, Eqs. (6) and (14), we can write

$$S_{\mathrm{cl}}=NZ^2\left[S_0(v)+n_{\mathrm{cl}}\int d^3r\, g_{\mathrm{cl}}(r)I(r,v)\right], \qquad (22)$$

and using Eq. (15) for $I(r,v)$ we can transform this as follows:

$$S_{\rm cl}=NZ^2\frac{2}{\pi v^2}\int_0^\infty\frac{dk}{k}[1+F_{\rm cl}(k)]\int_0^{kv}\omega\ d\omega\ {\rm Im}\left[\frac{-1}{\epsilon(k,\omega)}\right], \tag{23}$$

where $F_{\rm cl}(k)$ is given by Eq. (17).

Moreover, using Eqs. (8)–(12) for $g_{\rm cl}(r)$ we get

$$\begin{aligned}F_{\rm cl}(k)&=C_N\ n_{\rm cl}(2r_{\rm cl})^3 f_{\rm cl}(kr_0,2kr_{\rm cl})\\&=\frac{6}{\pi}NC_N f_{\rm cl}(kr_0,2kr_{\rm cl}),\end{aligned} \tag{24}$$

where we have replaced $n_{\rm cl}(2r_{\rm cl})^3=(6/\pi)N$, from Eq. (13).

The function $f_{\rm cl}(p,q)$ (where $p=kr_0$, $q=2kr_{\rm cl}$) is given by

$$f_{\rm cl}(p,q)=\int_{p/q}^1 4\pi x^2 dx\frac{\sin(qx)}{qx}\left(1-\frac{3}{2}x+\frac{1}{2}x^3\right), \tag{25}$$

and can be calculated analytically, with the result

$$\begin{aligned}\left(\frac{1}{4\pi}\right)f_{\rm cl}(p,q)=&[\tfrac{1}{2}p^4-\tfrac{3}{2}p^2(q^2+4)+pq^3+3q^2+12]q^{-6}\\&\times\cos(p)-[2p^3-3p(q^2+4)+q^3]q^{-6}\\&\times\sin(p)+3(q^2-4)q^{-6}\cos(q)\\&-12q^{-5}\sin(q).\end{aligned} \tag{26}$$

Then, we can write the cluster stopping power as in Eq. (6): $S_{\rm cl}=NZ^2[S_0(v)+I_{\rm cl}(v)]$, with

$$S_0(v)=\frac{2}{\pi v^2}\int_0^\infty\frac{dk}{k}\int_0^{kv}\omega\ d\omega\ \ {\rm Im}\left[\frac{-1}{\epsilon(k,\omega)}\right], \tag{27}$$

and

$$\begin{aligned}I_{\rm cl}(v)=&\left(\frac{6}{\pi}NC_N\right)\frac{2}{\pi v^2}\int_0^\infty\frac{dk}{k}f_{\rm cl}(kr_0,2kr_{\rm cl})\\&\times\int_0^{kv}\omega\ d\omega\ \ {\rm Im}\left[\frac{-1}{\epsilon(k,\omega)}\right].\end{aligned} \tag{28}$$

We will now derive the scaling laws for the cases of low and high velocities.

A. Low velocities

We can approximate the dielectric function by the low frequency limit [21], namely,

$${\rm Im}\left[\frac{-1}{\epsilon(k,\omega)}\right]\cong\left(\frac{2\pi}{k_BT}\right)^{3/2}\frac{n_Pk\omega}{(k^2+k_D^2)^2}, \tag{29}$$

with $k_D=1/\lambda_D=\omega_P/v_T$. Then from Eq. (28) we get

$$I_{\rm cl}\cong\frac{2n_Pv}{3\pi}\left(\frac{2\pi}{k_BT}\right)^{3/2}\int_0^\infty dk\frac{k^3F_{\rm cl}(k)}{(k^2+k_D^2)^2}. \tag{30}$$

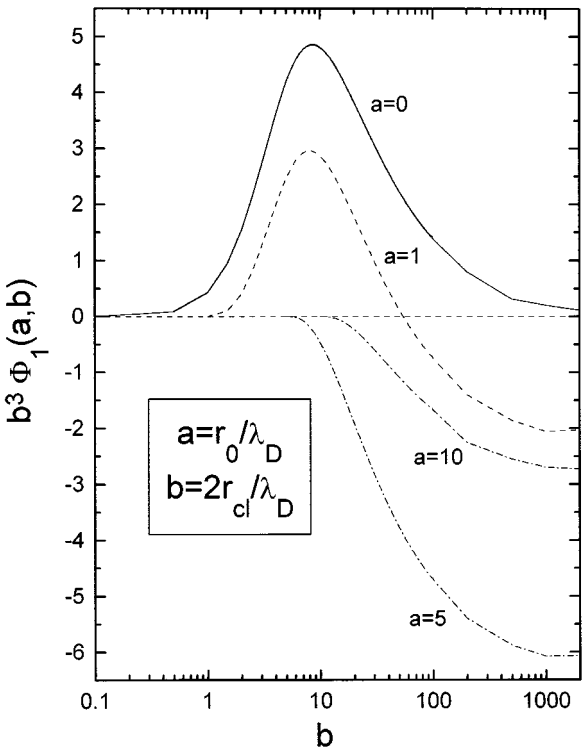

FIG. 5. Low-velocity scaling function $b^3\Phi_1(a,b)$, in Eqs. (33) and (35), for $a=0$, 1, 5, and 10, versus the variable b.

A similar expression is obtained for S_0, with $F_{\rm cl}(k)$ replaced by 1, which by integration yields

$$S_0\cong\frac{2n_Pv}{3\pi}\left(\frac{2\pi}{k_BT}\right)^{3/2}\ln\Lambda_1, \tag{31}$$

where $\ln\Lambda_1$ is given in this case by

$$\ln\Lambda_1=\int_0^{k_{\rm max}}\frac{k^3dk}{(k^2+k_D^2)^2}=\frac{1}{2}\left[\ln(1+X)-\frac{X}{(1+X)}\right], \tag{32}$$

with $X=(k_{\rm max}/k_D)^2$.

The value of $k_{\rm max}$ is given by [22] $k_{\rm max}=\min\{2mv_T/\hbar,\ k_BT/Ze^2\}$.

From Eq. (28) and using the same approximation, Eq. (29), we find the relation between the interference and the individual stopping terms:

$$\frac{I_{\rm cl}}{S_0}=\frac{6}{\pi}NC_N\frac{\Phi_1(a,b)}{\ln\Lambda_1}=C_Nn_{\rm cl}\lambda_D^3\frac{b^3\Phi_1(a,b)}{\ln\Lambda_1}, \tag{33}$$

where

$$\begin{aligned}a&=k_Dr_0=r_0\omega_P/v_T,\\b&=2k_Dr_{\rm cl}=2r_{\rm cl}\omega_P/v_T,\end{aligned} \tag{34}$$

and $\Phi_1(a,b)$ is the low-velocity scaling function, given by

$$\Phi_1(a,b)=\int_0^\infty\frac{x^3dx}{(x^2+1)^2}f_{\rm cl}(xa,xb). \tag{35}$$

The form of the function $b^3\Phi_1(a,b)$ is shown in Fig. 5.

We observe that for small values of a there exists a maximum at $b \cong 8.5$ (i.e., $r_{\rm cl} \sim 4\lambda_D$). Going back to Fig. 1(a) we find that this maximum corresponds to conditions such that most of the particles in the cluster interfere in a positive way. For larger values of b the situation is similar to the case $r_{\rm cl}=10\lambda_D$ in Fig. 1(a), where positive and negative contributions to the integral cancel partially, and the value of $b^3\Phi_1$ decreases. Figure 1(a) also serves to explain why the values of $\Phi_1(a,b)$ become negative with increasing values of a, due to a larger contribution from the negative part of the integrating function displayed in that figure.

The existence of an absolute maximum for $a=0$ in Fig. 5 is an important effect which will give place to a maximum in the energy loss of the whole cluster. The values corresponding to this maximum are the following:

$$b_{\rm max} \cong 8.5, \qquad [b^3\Phi_1(a,b)]_{\rm max} \cong 4.83. \tag{36}$$

B. High velocities

We can use in this case the so-called plasmon-pole approximation [18]:

$$\mathrm{Im}\left[\frac{-1}{\epsilon(k,\omega)}\right] \cong \frac{\pi}{2}\omega_P \delta(\omega-\omega_P). \tag{37}$$

Then, from Eqs. (27) and (28) we get

$$S_0(v) \cong \left(\frac{\omega_P}{v}\right)^2 \int_{\omega_P/v}^{k_{\rm max}} \frac{dk}{k} = \left(\frac{\omega_P}{v}\right)^2 \ln\Lambda_2 \tag{38}$$

and

$$I_{\rm cl}(v) \cong \frac{6}{\pi} N C_N \left(\frac{\omega_P}{v}\right)^2 \int_{\omega_P/v}^{\infty} \frac{dk}{k} f_{\rm cl}(kr_0, 2kr_{\rm cl}), \tag{39}$$

with $\ln\Lambda_2 = \ln(k_{\rm max}v/\omega_P)$, and the value of $k_{\rm max}$ is given in this case by [22] $k_{\rm max} = \min\{2mv/\hbar,\ mv^2/Ze^2\}$.

Therefore the I/S ratio now becomes

$$\frac{I_{\rm cl}}{S_0} = \frac{6}{\pi} N C_N \frac{\Phi_2(a,b)}{\ln\Lambda_2} = C_N n_{\rm cl} \lambda^3 \frac{b^3\Phi_2(a,b)}{\ln\Lambda_2}, \tag{40}$$

where now

$$a = r_0/\lambda = r_0\omega_P/v, \qquad b = 2r_{\rm cl}/\lambda = 2r_{\rm cl}\omega_P/v, \qquad \ln\Lambda_2 = \ln\left(\frac{k_{\rm max}v}{\omega_P}\right), \tag{41}$$

and $\lambda = v/\omega_P$.

The high-velocity scaling function $\Phi_2(a,b)$ is given by

$$\Phi_2(a,b) = \int_1^{\infty} \frac{dx}{x} f_{\rm cl}(xa, xb). \tag{42}$$

It should be noted that the integration limits in the Φ_1 and Φ_2 functions, Eqs. (35) and (42), have been extended to infinity [as well as in Eqs. (30) and (39)]. This is usually a good approximation in as much as $k_{\rm max}r \gg 1$ for all the particles in the cluster. Otherwise, the upper limits of integration in Eqs. (35) and (42) would be given by $k_{\rm max}v_T/\omega_P$ and $k_{\rm max}v/\omega_P$, respectively.

The form of the function $b^3\Phi_2(a,b)$ is shown in Fig. 6, which for clarity is split in two parts. The analysis of this figure is similar to the one given for Fig. 5.

The main maximum for $a=0$ in Fig. 6 is characterized by the values

$$b_{\rm max} \cong 3.6, \qquad [b^3\Phi_2(a,b)]_{\rm max} \cong 4.28. \tag{43}$$

The oscillatory effects observed now (nonexistent in the previous case of Fig. 5) are typical of the high-velocity regime, and arise from the oscillatory behavior of the dicluster function $I(r,v)$ in Fig. 1(b). The origin of this behavior is the wakelike characteristics of the induced potential arising from the excitation of collective modes (plasma waves) by fast particles ($v > v_T$).

Moreover, the results for $a=3$, 5, 8, and 10 in Fig. 6(b) show the importance of these oscillations even in the limit of very large clusters ($b \to \infty$). This limit will be discussed in the next section.

C. Infinite-cluster limit

Let us now consider the form of the scaling functions in the limit of very large clusters, namely, $b \gg 1$ (i.e., $r_{\rm cl} \gg v_T/\omega_P$ and v/ω_P, respectively).

Taking the limit $q \to \infty$ in Eq. (26) we get

$$f_{\rm cl}(p,q) \cong \left(\frac{4\pi}{q^3}\right)[p\ \cos(p) - \sin(p)]. \tag{44}$$

Using this in Eqs. (35) and (42) we find the corresponding limits:

$$\Phi_1(a,\infty) = \left(\frac{4\pi}{3}\right)\left(\frac{a}{b}\right)^3 \varphi_1(a), \tag{45}$$

$$\Phi_2(a,\infty) = \left(\frac{4\pi}{3}\right)\left(\frac{a}{b}\right)^3 \varphi_2(a), \tag{46}$$

where

$$\varphi_1(a) = \frac{3}{a^3}\int_0^{\infty} \frac{dx}{(x^2+1)^2}[ax\ \cos(ax) - \sin(ax)], \tag{47}$$

and

$$\varphi_2(a) = \frac{3}{a^3}\int_1^{\infty} \frac{dx}{x^4}[ax\ \cos(ax) - \sin(ax)]. \tag{48}$$

The latter integral can be calculated analytically, yielding

$$\varphi_2(a) = \mathrm{Ci}(a) + \frac{\cos(a)}{a^2} - \left(\frac{1}{a^3} + \frac{1}{a}\right)\sin(a), \tag{49}$$

in terms of the cosine integral function $\mathrm{Ci}(x)$.

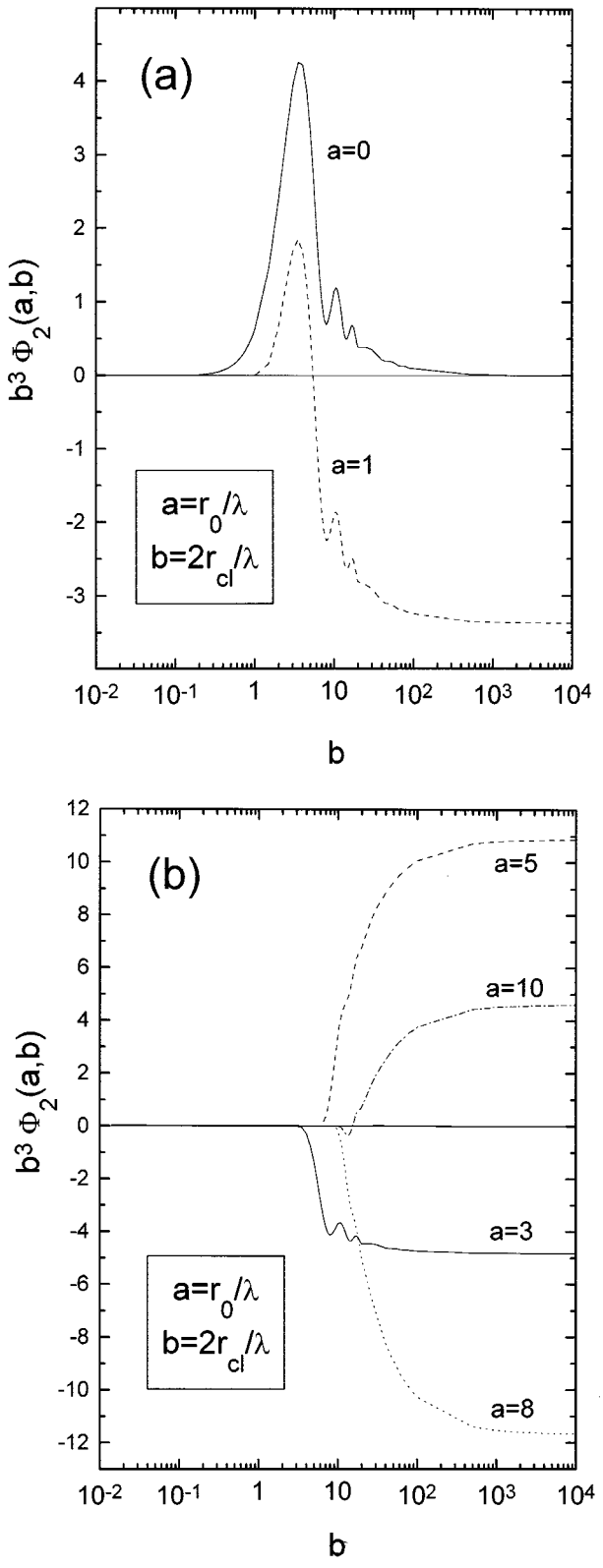

FIG. 6. High-velocity scaling function $b^3\Phi_2(a,b)$, in Eqs. (40) and (42), for $a=0$ and 1 [in (a)], and for $a=3$, 5, 8, and 10 [in (b)], as a function of the variable b.

Finally, using Eqs. (33), (40), (45), and (46), and replacing $(4\pi/3)n_{\rm cl}r_0^3=1$, Eq. (13), the I/S ratio takes now the following very simple forms.

1. Low-velocity case:

$$\frac{I_{\rm cl}}{S_0}\cong\frac{\varphi_1(a)}{\ln\Lambda_1}, \tag{50}$$

with $a=r_0/\lambda_D=r_0\omega_P/v_T$.

2. High-velocity case:

$$\frac{I_{\rm cl}}{S_0}\cong\frac{\varphi_2(a)}{\ln\Lambda_2}, \tag{51}$$

with $a=r_0/\lambda=r_0\omega_P/v$.

The functions $\varphi_1(a)$ and $\varphi_2(a)$ are shown in Fig. 7. Both functions are negative for $a<4$. Thus we find a rather unexpected result: the averaged interference effects for very large clusters are predominantly negative; this indicates that the positive interferences between closest neighbors are overtaken by the negative contributions from more distant neighbors (cf. Fig. 1).

The limit $a\gg1$, where both φ_1 and φ_2 functions vanish, corresponds to the limit of separated ions, interacting with the plasma without interfering among them.

We should finally note that the infinite-cluster limit as derived here requires both $b\gg1$ and $ab\gg1$. Actually, the second condition may become more difficult to achieve. For instance, using the values of Eq. (41), the condition $ab\gg1$ implies

$$2r_0r_{\rm cl}\gg(v/\omega_P)^2.$$

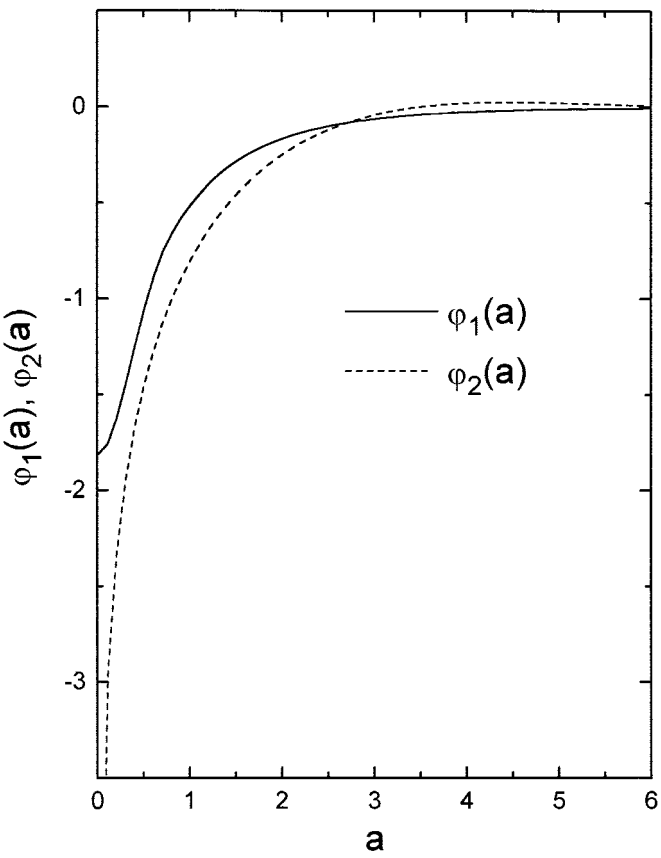

FIG. 7. Functions $\varphi_1(a)$ and $\varphi_2(a)$ in Eqs. (45)–(48), which determine the average interference effect for very large clusters, Eqs. (50) and (51).

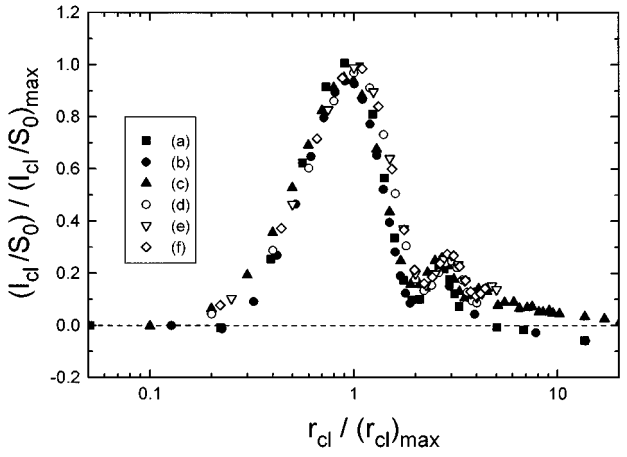

FIG. 8. I/S ratios numerically calculated from Eqs. (16) and (17) and scaled to the maximum values predicted by Eq. (53) for the high-velocity case. The data shown here were obtained from calculations in the following cases (densities given in cm^{-3}): (a) $n_P=10^{20}$, $n_{cl}=10^{16}$, $v=20$ a.u., (b) $n_P=10^{20}$, $n_{cl}=1.6\times10^{15}$, $v=35$ a.u., (c) $n_P=10^{18}$, $n_{cl}=10^{14}$, $v=20$ a.u., (d) $n_P=10^{16}$, $n_{cl}=10^{9}$, $v=60$ a.u., (e) $n_P=10^{14}$, $n_{cl}=10^{9}$, $v=10$ a.u., (f) $n_P=10^{12}$, $n_{cl}=10^{7}$, $v=20$ a.u.

For rather dense plasmas, where $\omega_P\sim0.1$–1 a.u., this condition may be fulfilled for reasonable cluster sizes (e.g., $r_{cl}>10^3$ a.u.). However, for dilute (MCF) plasmas, where $\omega_P\sim10^{-5}$ a.u., much larger clusters should be considered (e.g., $r_0\sim10^6$ a.u., $r_{cl}\sim10^9$ a.u., $v\sim10$ a.u.; then $a\sim1$, $b\sim1000$); the latter situation may be achieved if a whole bunch of particles (from a pulsed beam) is considered.

D. Resonant effect in cluster stopping power

Let us further analyze the conditions for a maximum enhancement of the cluster stopping power due to the collective interaction.

As shown before, the conditions to reach the maximum values in the energy loss are given by Eqs. (36) and (43), for low and high velocities, respectively. In terms of the physical parameters, and using Eqs. (34) and (41), these conditions read (i) low-velocity maximum:

$$r_{cl}^{max}=4.25\frac{v_T}{\omega_P}\equiv4.25\lambda_D,$$
$$\left(\frac{I_{cl}}{S_0}\right)_{max}=\frac{4.8}{\ln\Lambda}n_{cl}\lambda_D^3, \tag{52}$$

(ii) high-velocity maximum:

$$r_{cl}^{max}=1.8\frac{v}{\omega_P},$$
$$\left(\frac{I_{cl}}{S_0}\right)_{max}=\frac{4.3}{\ln\Lambda}n_{cl}\left(\frac{v}{\omega_P}\right)^3. \tag{53}$$

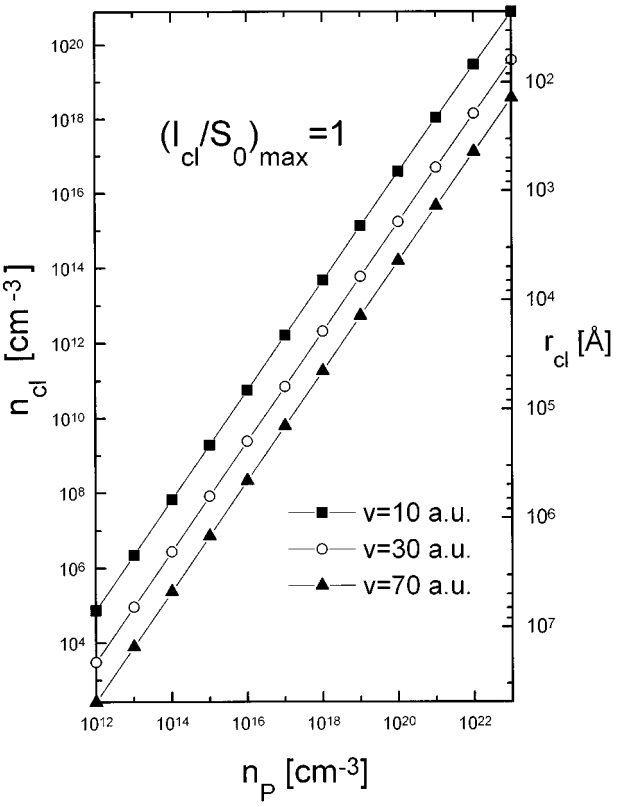

FIG. 9. Conditions required to obtain a 100% enhancement in the cluster energy loss. The figure shows the values of the cluster density n_{cl} (left scale) and cluster radius r_{cl} (right scale), as given by Eq. (53) for the case $(I_{cl}/S_0)=1$, with plasma densities n_P ranging from 10^{12} to 10^{23} cm^{-3}.

In both cases we have set $C_N\cong1$, which is a very good approximation for large clusters [$N\gg1$, $r_0\ll2r_{cl}$, see Eq. (12)].

In a previous paper [17] we have numerically approximated the stopping power maximum in the case of high velocities, in the form $r_{cl}^{max}\approx2v/\omega_P$, $(I_{cl}/S_0)_{max}\approx(\frac{1}{3})n_{cl}(v/\omega_P)^3$. We can now understand the origin of these approximations in terms of the more general scaling properties derived here. The conditions for the high-velocity maximum are given by the more accurate values of Eq. (53). The factor $\frac{1}{3}$ previously reported is only a rough approximation to $4.3/\ln\Lambda$, with $\ln\Lambda\cong12\pm2$, as can be found for the cases calculated in Ref. [17].

The calculations reported previously [17], together with several new cases, have been rescaled and presented in Fig. 8, according to the predictions of Eq. (53), in order to illustrate the applicability of the scaling relations. We note that the cases presented in this figure cover very wide ranges of cluster and plasma densities ($n_{cl}\sim10^7$–10^{16} cm^{-3}, $n_P\sim10^{12}$–10^{20} cm^{-3}), and they are all contained in the present formulation.

As a final question we address now the problem of possible applications of this effect in plasma heating experiments or fusion research. Let us consider for definiteness the conditions required to obtain an enhancement effect of $\sim100\%$ in the energy loss, i.e., $(I_{cl}/S_0)_{max}\sim1$. Using Eq. (53) we can determine the values of the cluster parameters corresponding to this case. In Fig. 9 we show the relevant

parameters, cluster density n_{cl} (on the left scale), and cluster size r_{cl} (on the right scale) for a wide range of plasma densities n_P and for velocities $v=10$, 30, and 70 a.u.

As may be observed, in the range of interest for tokamak experiments ($n_P \sim 10^{12}$–10^{14} cm^{-3}) the conditions may be achieved with particle bunches of sizes ~ 0.1 cm and densities $n_{cl} \sim 10^3$–10^5 cm^{-3} [of course, if higher cluster densities were used the enhancement effect should still be larger, provided that the cluster radius satisfies the resonant criterion, as predicted by Eq. (53)]. On the other hand, we find that for applications to ICF experiments ($n_P \sim 10^{22}$–10^{23} cm^{-3}) it would be necessary to use very compact clusters ($n_{cl} \sim 10^{18}$–10^{21} cm^{-3}, $r_{cl} \sim 20$–100 Å); these conditions may be fulfilled using large molecular-ion clusters, a case that is currently being considered and has also been explored in various recent publications [16,20,23].

V. SUMMARY AND CONCLUSIONS

The energy loss of large ion clusters in plasmas has been studied, with particular interest in a theoretical understanding of the general properties, and the derivation of analytical expressions to describe the results in terms of a few scaling functions.

Different cases have been considered in order to characterize the range of parameters where either vicinage effects (i.e., interactions between close neighbors) or the stronger collective effects (where all the particles in the cluster interact in a coherent way) become dominant.

The study of the scaling properties was performed for the cases of low and high velocities, through the derivation of appropriate scaling functions, $\Phi_1(a,b)$ and $\Phi_2(a,b)$, Eqs. (35) and (42), which depend on the main parameters of the beam and the plasma through the dimensionless variables a and b [Eqs. (34) and (41)]. The ratios between the interference term I_{cl} and the individual stopping term S_0 are given in similar ways by Eqs. (33) and (40), for each case.

A maximum enhancement of the cluster energy loss is obtained in the regime of strong collective effects, both for low and high velocities, when the parameters satisfy the conditions for maximum coherent interference for the whole cluster. These conditions can be cast in the form of Eqs. (52) and (53), respectively.

We find that these collective effects can modify the energy loss of ion clusters or very intense ion beams in plasmas, in cases of interest for MCF and ICF studies as well as in experiments using pinched or focused plasmas. Several examples have been given in a previous paper [17].

Hence we expect that the general properties and scaling laws derived in this paper will be useful in a wide range of cases or applications pertaining to collective effects in beam-plasma interactions.

ACKNOWLEDGMENTS

This work was partially supported by Consejo Nacional de Investigaciones Científicas *y* Técnicas (CONICET, Argentina) through a research grant (PID Grant No. 300192).

[1] E. Speth, Rep. Prog. Phys. **52**, 57 (1989).
[2] J. D. Strachan *et al.*, Phys. Rev. Lett. **72**, 3526 (1994).
[3] S. Humphries, Nucl. Fusion **20**, 1549 (1980).
[4] C. Deutsch, Ann. Phys. (Paris) **11**, 1 (1986).
[5] R. C. Arnold and J. Meyer-ter-Vehn, Rep. Prog. Phys. **50**, 559 (1987).
[6] C. Deutsch and N. A. Tahir, Phys. Fluids B **4**, 3735 (1992).
[7] W. Brandt, A. Ratkowsky, and R. H. Ritchie, Phys. Rev. Lett. **33**, 1325 (1974).
[8] N. R. Arista and V. H. Ponce, J. Phys. C **8**, L188 (1975).
[9] N. R. Arista, Phys. Rev. B **18**, 1 (1978).
[10] G. Basbas and R. H. Ritchie, Phys. Rev. A **25**, 1943 (1982).
[11] R. A. McCorkle and G. J. Iafrate, Phys. Rev. Lett. **39**, 1263 (1977).
[12] D. W. Rule and M. H. Cha, Phys. Rev. A **24**, 55 (1981).
[13] D. W. Rule and O. H. Crawford, Phys. Rev. Lett. **52**, 934 (1984).
[14] C. Deutsch, Laser Part. Beams **8**, 55 (1981).
[15] J. D'Avanzo, M. Lontano, and P. F. Bortignon, Phys. Rev. A **45**, 6126 (1992); Phys. Rev. E **47**, 3574 (1993).
[16] E. Nardi, Z. Zinamon, and D. Ben-Hamu, Nuovo Cimento A **106**, 1839 (1993).
[17] E. Bringa and N. R. Arista, Phys. Rev. E **52**, 3010 (1995).
[18] P. M. Echenique, R. H. Ritchie, and W. Brandt, Phys. Rev. B **20**, 2567 (1979).
[19] E. Bringa and N. R. Arista, Phys. Rev. E **54**, 4101 (1996).
[20] I. Abril, M. Vicanek, A. Gras-Martí, and N. R. Arista, Nucl. Instrum. Methods B **67**, 56 (1992); M. Vicanek, I. Abril, N. R. Arista, and A. Gras-Martí, Phys. Rev. A **46**, 5745 (1992).
[21] J. Ichimaru, *Basic Principles of Plasma Physics* (Benjamin, New York, 1973).
[22] L. de Ferrariis and N. R. Arista, Phys. Rev. A **29**, 2145 (1984).
[23] C. Deutsch and P. Fromy, Phys. Rev. E **51**, 632 (1995).